Scilight

Photocatalysis
https://www.sciltp.com/journals/photocatalysis

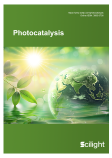

Supplementary Materials

Photocatalytic Uphill Reactions with Apparent Quantum Efficiency over 10%

Liang Tian, Alberto García-Baldoví * and Hermenegildo García *

Instituto de Tecnología Química, Universitat Politècnica de València-Consejo Superior de Investigaciones Científicas, Universitat Politècnica de València, Av. de los Naranjos s/n, 46022 Valencia, Spain
* Correspondence: algarbal@itq.upv.es (A.G.-B.); hgarcia@qim.upv.es (H.G.)

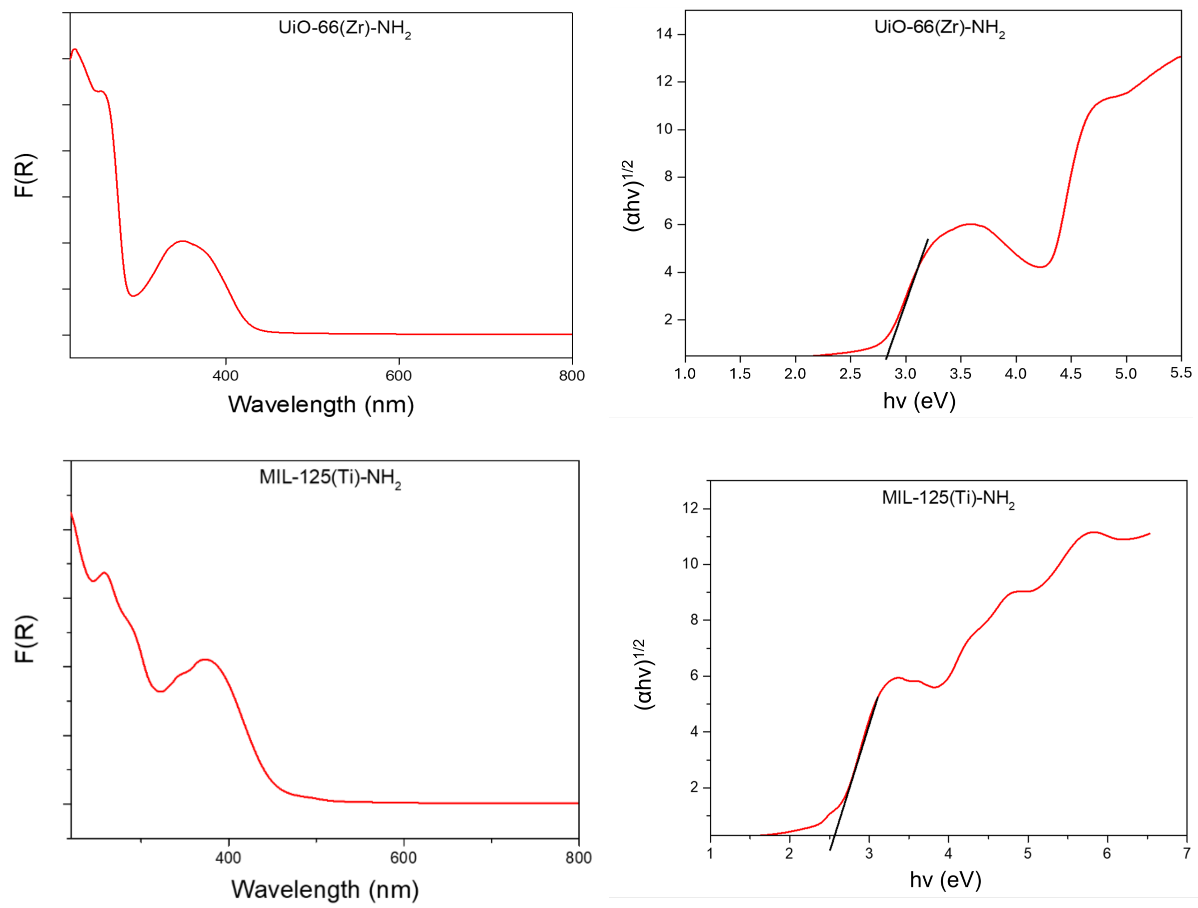

Figure S1. Diffuse reflectance spectra and corresponding Tauc plots of UiO-66(Zr)-NH_2 and MIL-125(Ti)-NH_2 photocatalysts.

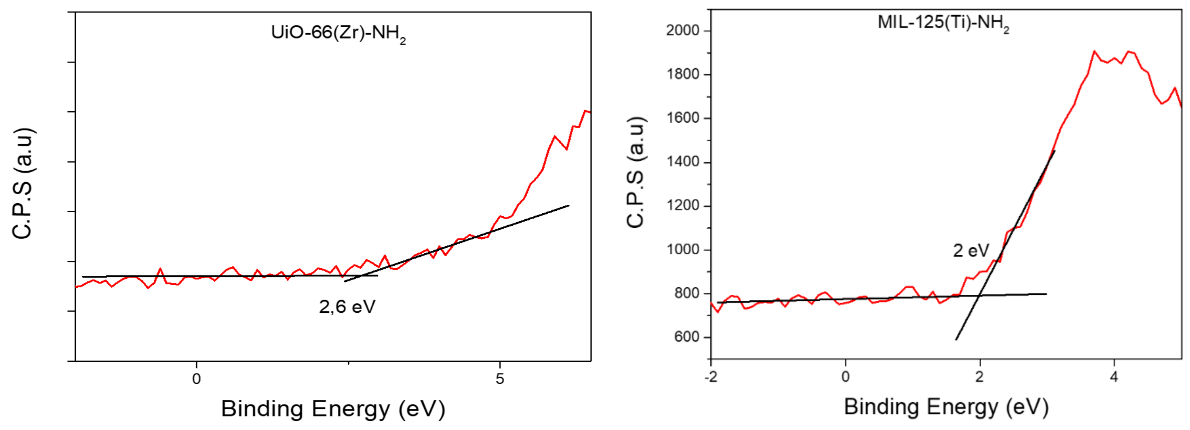

Figure S2. Valence band edge positions determined from the onset of photoelectron emission in XPS spectra, corrected by the instrument work function, for UiO-66(Zr)-NH_2 and MIL-125(Ti)-NH_2.

UiO-66(Zr)-NH_2

MIL-125(Ti)-NH_2

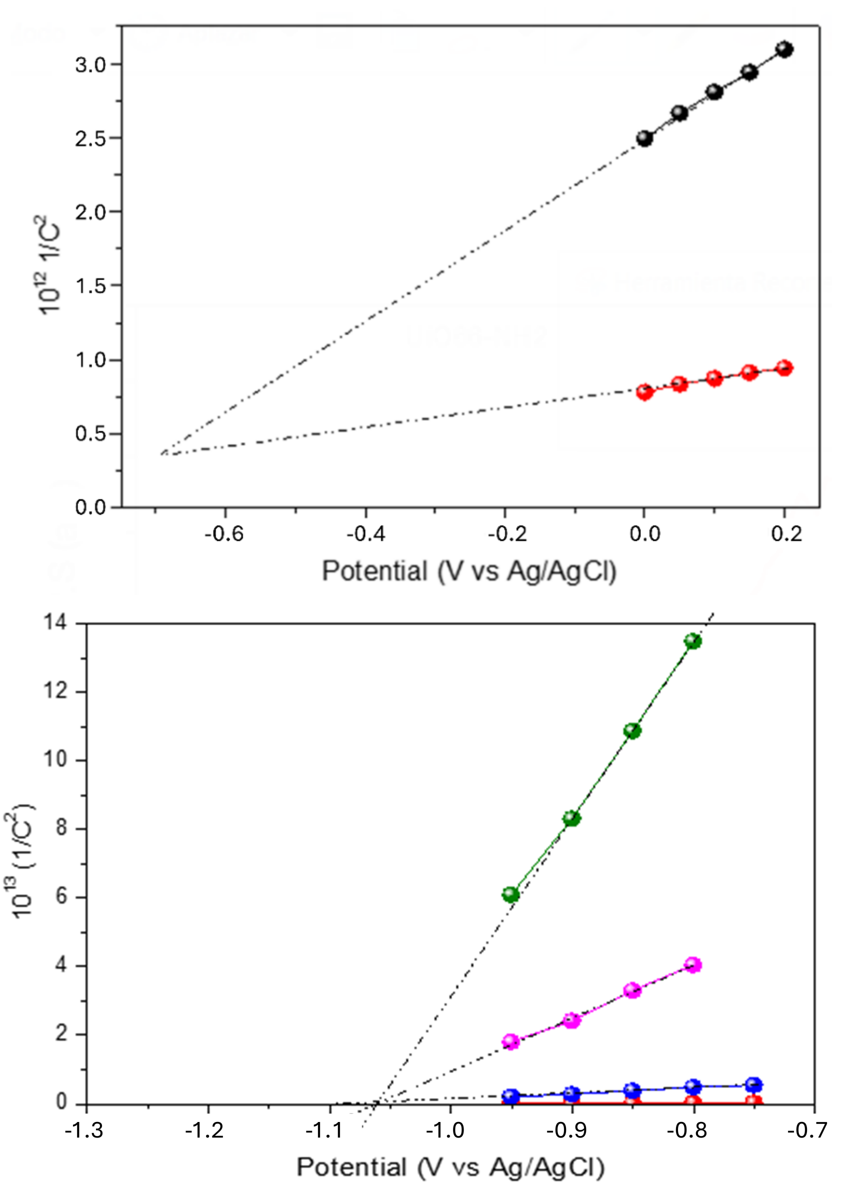

Figure S3. Mott–Schottky plots from electrochemical impedance spectroscopy used to estimate the conduction band potentials of UiO-66(Zr)-NH_2 (working frequencies: 100 Hz, red; 500 Hz, black) and MIL-125(Ti)-NH_2 (working frequencies: 100 Hz, red; 150 Hz, blue; 500 Hz, violet; 1000 Hz, green).

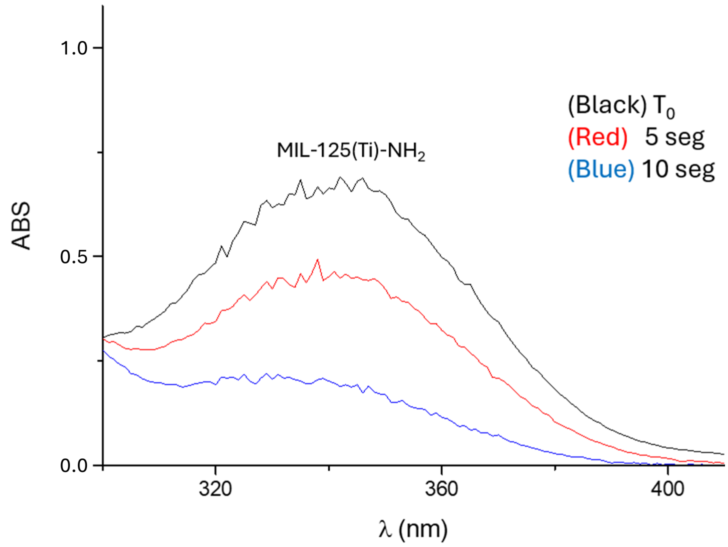

Figure S4. Optical spectra in the near-UV region showing the disappearance of the characteristic NADH absorption band at λ_{max} 340 nm upon photoxidation.

Figure S5. Photograph of the photocatalytic set up used to determine apparent quantum yields in the present study.

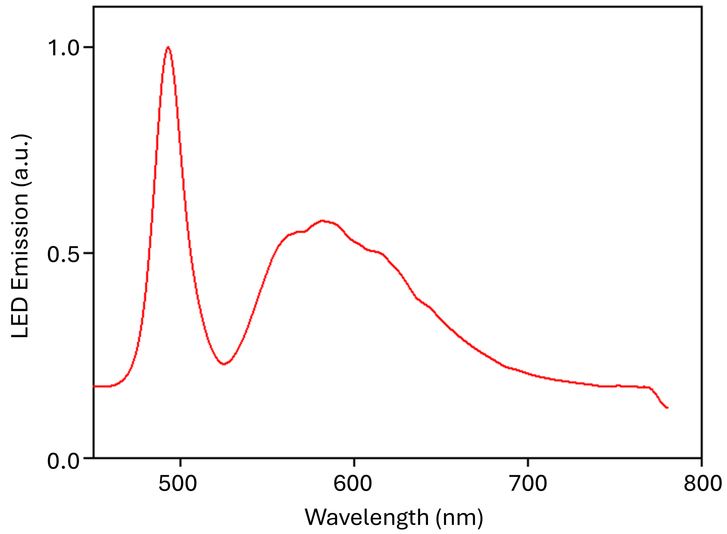

Figure S6. Emission spectrum of white LED used as light source of visible light. The total emission intensity used in the present study is 0.3 mW cm^{-2}.

Table S1. Comparison of the apparent quantum yields (AQY) of various reported photocatalytic systems with the values achieved in the present study**.**

Catalysts	Reaction	AQY	Ref.
UiO-66(Zr)-NH_2	Reduction reaction of $[C_{12}H_{14}N_2]^{2+}$ mediators	>90% at 450 nm	This work
	Reduction reaction of $[C_{12}H_{12}N_2]^{2+}$ mediators	<1% at 450 nm	
	Reduction reaction of $[C_{13}H_{14}N_2]^{2+}$ mediators	1 ± 1% at 450 nm	
MIL-125(Ti)-NH_2	Reduction reaction of $[C_{12}H_{14}N_2]^{2+}$ mediators	88 ± 5% at 450 nm	
	Reduction reaction of $[C_{12}H_{12}N_2]^{2+}$ mediators	2 ± 2% at 450 nm	
	Reduction reaction of $[C_{13}H_{14}N_2]^{2+}$ mediators	Too low at 450 nm	
UiO-66(Zr)-NH_2	Oxidation reaction of $Fe(CN)_6^{4+}$ mediators	67 ± 5% at 450 nm	
	Oxidation reaction of NADH mediators	30 ± 5% at 450 nm	
MIL-125(Ti)-NH_2	Oxidation reaction of $Fe(CN)_6^{4+}$ mediators	64 ± 5% at 450 nm	
	Oxidation reaction of NADH mediators	Too low at 450 nm	
Rh/$Cr_2O_3^{-}$ Ta_3N_5 /$KTaO_3$	overall water splitting	2.2% at 320 nm; 0.22% at 420 nm; 0.024% at 500 nm	[1]
Rh/$Cr_2O_3^{-}$ $Y_2Ti_2O_5S_2$	H_2 production	5.3 ± 0.3% at 420−480 nm	[2]
IrO_2/$Y_2Ti_2O_5S_2$	O_2 production	2.3 ± 0.1% at 420−480 nm	[2]
Al-$SrTiO_3$	Overall water splitting	14.8% at 375nm	[3]
NiO/$NaTaO_3$:La	Overall water splitting	56% at 270 nm	[4]
$RhCrO_x$/$SrTiO_3$	Overall water splitting	56% at 365 nm	[5]
CoO_x/Mo:$BiVO_4$/(Ag/Pd)	H_2O_2 production	13.1% at 420 nm; ~7.5% at 490nm; ~0% at 590nm	[6]
HEP-TAPT-COF	H_2O_2 production	15.35% at 420 nm; 14.98% at 450 nm; 9.63% at 500nm; 4.37% at 550 nm; 1.92% at 600 nm	[7]

Reference

1. Wang, Z.; Inoue, Y.; Hisatomi, T.; et al. Overall water splitting by Ta_3N_5 nanorod single crystals grown on the edges of $KTaO_3$ particles. *Nat. Catal.* **2018**, *1*, 756–763.
2. Wang, Q.; Nakabayashi, M.; Hisatomi, T.; et al. Oxysulfide photocatalyst for visible-light-driven overall water splitting. Nature *materials* **2019**, *18*, 827–832.
3. Zhao, Z.; Goncalves, R.V.; Barman, S.K.; et al. Electronic structure basis for enhanced overall water splitting photocatalysis with aluminum doped $SrTiO_3$ in natural sunlight. *Energy Environ. Sci.* **2019**, *12*, 1385–1395.
4. Kato, H.; Asakura, K.; Kudo, A. Highly efficient water splitting into H_2 and O_2 over lanthanum-doped $NaTaO_3$ photocatalysts with high crystallinity and surface nanostructure. *J. Am. Chem. Soc.* **2003**, *125*, 3082–3089.
5. Goto, Y.; Hisatomi, T.; Wang, Q.; et al. A particulate photocatalyst water-splitting panel for large-scale solar hydrogen generation. *Joule* **2018**, *2*, 509–520.
6. Liu, T.; Pan, Z.; Kato, K.; et al. A general interfacial-energetics-tuning strategy for enhanced artificial photosynthesis. *Nat. Commun.* **2022**, *13*, 7783.
7. Chen, D.; Chen, W.; Wu, Y.; et al. Covalent organic frameworks containing dual O_2 reduction centers for overall photosynthetic hydrogen peroxide production. *Angew. Chem. Int. Ed.* **2023**, *62*, e202217479.